

# Investigation of Silver-Containing Layered Materials and Their Interactions with Primary Amines Using Solid-State $^{109}\text{Ag}$ and $^{15}\text{N}$ NMR Spectroscopy and First Principles Calculations

Hiyam Hamaed,<sup>†</sup> Andy Y. H. Lo,<sup>†</sup> Leslie J. May,<sup>‡</sup> Jared M. Taylor,<sup>‡</sup> George H. Shimizu,<sup>\*,‡</sup> and Robert W. Schurko<sup>\*,†</sup>

Department of Chemistry and Biochemistry, University of Windsor, Windsor, Ontario, Canada N9B 3P4, and Department of Chemistry, University of Calgary, Calgary, Alberta, Canada T2N 1N4

Received August 13, 2008

Silver-containing layered networks of the form  $[\text{Ag}(\text{L})]$  ( $\text{L} = 4\text{-pyridinesulfonate}$  or  $p\text{-toluenesulfonate}$ ) were treated with primary amines in different ratios. The structures of the parent supramolecular networks are well-known; however, their interactions with primary amines lead to the formation of new layered materials for which single-crystal X-ray structures cannot be obtained. Solid-state  $^{109}\text{Ag}$ ,  $^{15}\text{N}$ , and  $^{13}\text{C}$  cross-polarization magic-angle spinning (CP/MAS) NMR experiments, in combination with powder X-ray diffraction experiments and ab initio calculations, are utilized to investigate the interactions between the primary amines and the parent materials, and to propose structural models for the new materials.  $^{109}\text{Ag}$  chemical shift (CS) tensor parameters are extremely sensitive to changes in silver environments; hence,  $^1\text{H}\text{-}^{109}\text{Ag}$  CP/MAS NMR experiments are used to distinguish and characterize silver sites. The combination of  $^{109}\text{Ag}$  and  $^{15}\text{N}$  NMR experiments on starting materials and samples prepared with both  $^{15}\text{N}$ -labeled and unlabeled amines permits the accurate measurements of indirect  $^1\text{J}(^{109}\text{Ag}, ^{15}\text{N})$  and  $^1\text{J}(^{109}\text{Ag}, ^{14}\text{N})$  spin–spin coupling constants, providing further information on structure and bonding in these systems. First principles calculations of silver CS tensors and  $^1\text{J}(^{109}\text{Ag}, ^{14}\text{N})$  coupling constants in model complexes aid in formulating the proposed structural models for the new materials, which are largely comprised of layers of silver-diamine cations.

## Introduction

Coordination network materials, also referred to as metal-organic frameworks, represent a compromise between wholly inorganic and organic solids, often having the chemical and physical properties of the individual building blocks, as well as new properties that result from their connectivity.<sup>1–6</sup> Solid silver sulfonates are representative of this subtle balance, as

they are able to form stable layered networks composed of sulfonate bridges between silver ions.<sup>7–12</sup> The flexibility of their coordination chemistry and the adaptability of their lamellar structures enable the possibilities of selective reactivity or absorption of guest molecules.<sup>13–15</sup>

Shimizu and co-workers recently reported the synthesis and characterization of several new layered materials formed by the reaction of silver sulfonates with primary amines;<sup>13,15</sup>

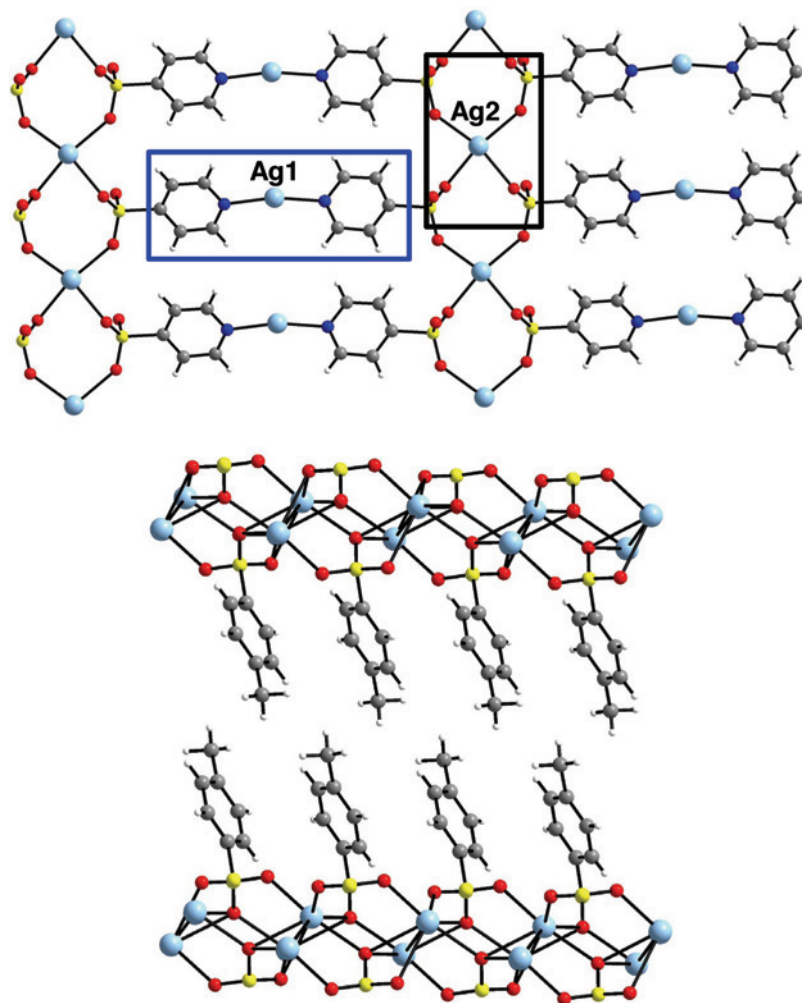
\* Authors to whom correspondence should be addressed. Phone: (519) 253-3000x3548 (R.W.S.); (403) 220-5347(G.H.S.). Fax: (519) 973-7098 (R.W.S.); (403) 289-9488 (G.H.S.). E-mail: rschurko@uwindsor.ca (R.W.S.); gshimizu@ucalgary.ca (G.H.S.).

<sup>†</sup> University of Windsor.

<sup>‡</sup> University of Calgary.

- (1) Kitagawa, S.; Kitaura, R.; Noro, S.-I. *Angew. Chem., Int. Ed.* **2004**, *43*, 2334.
- (2) Bradshaw, D.; Claridge, J. B.; Cussen, E. J.; Prior, T. J.; Rosseinsky, M. J. *Acc. Chem. Res.* **2005**, *38*, 273.
- (3) Janiak, C. *Dalton Trans.* **2003**, 2781.
- (4) Eddaoudi, M.; Kim, J.; Rosi, N.; Vodak, D.; Wachter, J.; O’Keeffe, M.; Yaghi Omar, M. *Science* **2002**, *295*, 469.
- (5) Yaghi, O. M.; O’Keeffe, M.; Ockwig, N. W.; Chae, H. K.; Eddaoudi, M.; Kim, J. *Nature* **2003**, *423*, 705.

- (6) Maspoch, D.; Ruiz-Molina, D.; Wurst, K.; Domingo, N.; Cavallini, M.; Biscarini, F.; Tejada, J.; Rovira, C.; Veciana, J. *Nat. Mater.* **2003**, *2*, 190.
- (7) Hoffart, D. J.; Dalrymple, S. A.; Shimizu, G. K. H. *Inorg. Chem.* **2005**, *44*, 8868.
- (8) Cote, A. P.; Shimizu, G. K. H. *Inorg. Chem.* **2004**, *43*, 6663.
- (9) Melcer, N. J.; Enright, G. D.; Ripmeester, J. A.; Shimizu, G. K. H. *Inorg. Chem.* **2001**, *40*, 4641.
- (10) Shimizu, G. K. H.; Enright, G. D.; Ratcliffe, C. I.; Preston, K. F.; Reid, J. L.; Ripmeester, J. A. *Chem. Commun.* **1999**, 1485.
- (11) Shimizu, G. K. H.; Enright, G. D.; Ratcliffe, C. I.; Ripmeester, J. A. *Chem. Commun.* **1999**, 461.
- (12) Shimizu, G. K. H.; Enright, G. D.; Ratcliffe, C. I.; Ripmeester, J. A.; Wayner, D. D. M. *Angew. Chem., Int. Ed.* **1998**, *37*, 1407.

**Scheme 1.** Schematic Representation of the Crystal Structures of [Ag(4-pyridinesulfonate)]<sub>4</sub> (**1a**, top) and [Ag(*p*-toluenesulfonate)] (**2a**, bottom)<sup>a</sup>

<sup>a</sup> There are two silver sites in **1a** and only one site in **2a**.

interestingly, layered solids were not produced in reactions of silver sulfonates with any other class of organic reactants. It was proposed that the new layered materials were likely formed from the intercalation of primary amines, on the basis of interlayer distances determined by powder X-ray diffraction (XRD). After publication of this study, several questions arose regarding the nature of these materials and the mechanism behind their synthesis. First, does the formation of these new materials actually result from the intercalation of primary amines? Second, are there selective interactions between the silver atoms and amine nitrogen atoms? Finally, can a combination of XRD methods and solid-state NMR of silver and nitrogen sites in these materials lend insight into their structures and the nature of their formation? While detailed crystal structures are available for the silver sulfonate starting materials (Scheme 1), they are not available for many intercalation or layered solids, since most often the samples have long-range disorder and suitably sized single crystals

cannot be isolated. Solid-state NMR (SSNMR) represents a powerful complementary tool for the characterization of structure, connectivity, and dynamics in such systems; most notably, the understanding of metal–ligand bonding interactions is crucial for the future rational design of such materials.

While <sup>15</sup>N NMR experiments on solid materials have become increasingly routine, solid-state silver NMR spectroscopy is infrequently applied despite the regular occurrence and significance of silver sites in a variety of technologically important materials.<sup>16–22</sup> This is partly due to the fact that <sup>107</sup>Ag and <sup>109</sup>Ag (both spin-1/2) have low gyromagnetic ratios ( $\gamma$ ) and correspondingly low receptivities (0.198 and 0.28, respectively, compared to <sup>13</sup>C). In addition, <sup>107/109</sup>Ag nuclei in solids often have exceedingly large

- (13) Shimizu, G. K. H.; Enright, G. D.; Ratcliffe, C. I.; Rego, G. S.; Reid, J. L.; Ripmeester, J. A. *Chem. Mater.* **1998**, *10*, 3282.  
 (14) Cote, A. P.; Ferguson, M. J.; Khan, K. A.; Enright, G. D.; Kulynych, A. D.; Dalrymple, S. A.; Shimizu, G. K. H. *Inorg. Chem.* **2002**, *41*, 287.  
 (15) May, L. J.; Shimizu, G. K. H. *Chem. Mater.* **2005**, *17*, 217.

- (16) Fijolek, H. G.; Oriskovich, T. A.; Benesi, A. J.; Gonzalez-Duarte, P.; Natan, M. J. *Inorg. Chem.* **1996**, *35*, 797.  
 (17) Fijolek, H. G.; Gonzalez-Duarte, P.; Park, S. H.; Suib, S. L.; Natan, M. J. *Inorg. Chem.* **1997**, *36*, 5299.  
 (18) Mustarelli, P.; Tomasi, C.; Quartarone, E.; Magistris, A.; Cutroni, M.; Mandanici, A. *Phys. Rev. B* **1998**, *58*, 9054.  
 (19) Rammial, T.; Abernethy, C. D.; Spicer, M. D.; McKenzie, I. D.; Gay, I. D.; Clyburne, J. A. C. *Inorg. Chem.* **2003**, *42*, 1391.  
 (20) Penner, G. H.; Li, W. *Solid State Nucl. Magn. Reson.* **2003**, *23*, 168.  
 (21) Penner, G. H.; Li, W. *Inorg. Chem.* **2004**, *43*, 5588.  
 (22) Bowmaker, G. A.; Harris, R. K.; Assadollahzadeh, B.; Apperley, D. C.; Hodgkinson, P.; Amornsakchai, P. *Magn. Reson. Chem.* **2004**, *42*, 819.

longitudinal relaxation time constants ( $T_1$ ), which may be on the order of minutes to hours, making the acquisition of high-quality  $^{109}\text{Ag}$  NMR spectra very challenging.<sup>22,23</sup> Further, NMR experiments on low- $\gamma$  nuclei (e.g.,  $\nu_0 = 18.67$  MHz at 9.4 T) are plagued by acoustic probe ringing, resulting in interference in the NMR free induction decay (FID), which partially or wholly obliterates the signal.

The cross-polarization magic-angle spinning (CP/MAS) experiment can address the sensitivity problems stemming from poor receptivity and long relaxation times; however, there must be spatially proximate, dipolar-coupled, abundant nuclei present (e.g.,  $^1\text{H}$ ,  $^{19}\text{F}$ , etc.).<sup>24,25</sup> The experimental time can be reduced due to the signal enhancement from CP (e.g., the maximum theoretical signal-to-noise ratio (S/N) enhancement factor for  $^1\text{H}$ - $^{109}\text{Ag}$  CP/MAS NMR experiments is proportional to  $\gamma(^1\text{H})/\gamma(^{109}\text{Ag}) = 21.7$ ) and the use of shorter recycle delays, since the CP/MAS NMR experiment depends on the  $T_1$  of the abundant spin (which is typically much smaller than that of  $^{109}\text{Ag}$ ). If higher spinning speeds are required or weaker dipolar couplings are present, the variable-amplitude CP (VACP) or RAMP-CP experiments can be used to obtain the optimal CP signal.<sup>26–30</sup> However, all of the CP experiments place a significant amount of stress on the solid-state NMR probes, since long contact times of 30 ms or more are often needed to obtain reasonable CP to the low- $\gamma$  silver nuclides. The use of silver NMR is continuing to increase, due to the availability of new hardware for low- $\gamma$  nuclei,<sup>31,32</sup> the development of pulse sequences for S/N enhancement,<sup>33–35</sup> and the recent proliferation of ultra-high-field NMR spectrometers.<sup>36–40</sup>

Herein, we report upon the application of solid-state  $^{109}\text{Ag}$ ,  $^{15}\text{N}$ , and  $^{13}\text{C}$  NMR experiments to the study of the molecular

structures of silver-containing layered materials. The silver-containing systems include  $[\text{Ag}(4\text{-pyridinesulfonate})]_4$  (**1a**); four samples of **1a** reacted with  $\text{C}_{12}\text{H}_{25}\text{NH}_2$  in different ratios, 1:0.5, 1:1, 1:1.5, and 1:2 (**1b**, **1c**, **1d**, and **1e**, respectively, where **1c** and **1e** were synthesized with 98% isotopically enriched  $\text{C}_{12}\text{H}_{25}^{15}\text{NH}_2$ );<sup>15</sup>  $[\text{Ag}(p\text{-toluenesulfonate})]$  (**2a**);<sup>13</sup> **2a** reacted with  $\text{C}_{12}\text{H}_{25}\text{NH}_2$  and  $\text{C}_9\text{H}_{19}\text{NH}_2$  in a 1:2 ratio (**2b** and **2c**, respectively);<sup>13</sup> and  $[\text{Ag}(\text{C}_{12}\text{H}_{25}\text{NH}_2)_2]^+[\text{NO}_3]^-$  (**3**).<sup>41</sup> Due to the extreme sensitivity of silver chemical shift (CS) tensors to structural changes,<sup>42</sup>  $^{109}\text{Ag}$  NMR experiments can be used to probe structural differences between starting materials and amine-containing samples.  $^{109}\text{Ag}$  and  $^{15}\text{N}$  NMR experiments on systems synthesized with  $^{15}\text{N}$ -enriched dodecylamine are used to identify the nature of the silver–nitrogen interactions, since they are crucial in the formation of these materials.<sup>43</sup> Finally, ab initio calculations of silver and nitrogen chemical shielding tensors, as well as one-bond  $^{109}\text{Ag}$ - $^{14/15}\text{N}$   $J$ -couplings, are presented to aid in proposing a tentative structural model for these new materials.

## Experimental Section

All chemicals were purchased from Sigma Aldrich Chemical Co. and used as received. The 98% enriched  $^{15}\text{N}$ -dodecylamine was purchased from Cambridge Isotope Laboratories. C, N, and H chemical analyses were obtained on a Control Equipment Corporation Model 440 system, with samples weighed in an ambient laboratory atmosphere. FT-IR data were obtained from KBr pellets on a Nicolet Nexus 470 Fourier transform spectrometer. Differential scanning calorimetry/thermogravimetric analysis (DSC/TGA) experiments were carried out on a Netzsch 449C Simultaneous Thermal Analyzer in a nitrogen atmosphere. Samples (ca. 5 mg) were placed in aluminum pans and referenced against an empty pan for the DSC measurements. Typical heating programs involved data collection between 25 and 450 °C with heating rates of 5 °C/min.

**Synthesis of Alkylamine Materials. Synthesis of 1b–1e.** An appropriate stoichiometric amount of dodecylamine (unlabeled or 98%  $^{15}\text{N}$ -enriched) was dissolved in diethyl ether and added to **1a** suspended in diethyl ether (e.g., for **1c**, 1.0 mmol of dodecylamine was added per silver center to produce the 1:1 complex). The heterogeneous mixture was stirred for 6 h, after which the ether was removed by filtration. No uptake of diethyl ether by the host was observed in either the presence or absence of amine molecules (as determined by powder XRD and simultaneous thermal analysis). Samples of **1a**, **2b**, **2c**, and **3** were synthesized as described in the literature.<sup>13,15,41</sup>

**$[\text{Ag}(4\text{-pyridinesulfonate})]_4$  Reacted with  $\text{C}_{12}\text{H}_{25}\text{NH}_2$  in 1:0.5, 1b.** Yield: 95%. Anal. calcd for  $\text{AgC}_{11}\text{H}_{17.5}\text{N}_{1.5}\text{SO}_3$  (357.51 g/mol): C, 36.83; H, 4.92; N, 5.86. Found: C, 36.12; H, 4.66; N, 5.68. DSC/TGA: 97 °C (11.8 J g<sup>-1</sup>, endo), 132 °C (28.5 J g<sup>-1</sup>, endo), 145–215 °C (68.5 J g<sup>-1</sup>, exo), 210–280 °C (112.5 J g<sup>-1</sup>, endo), –8.5% obsd and –25.6% calcd for a loss of 0.5 equiv  $\text{C}_{12}\text{H}_{25}\text{NH}_2$  in the first two mass losses combined, 290–410 °C (114.2 J g<sup>-1</sup>, endo, 5.5 J g<sup>-1</sup>, endo), loss of the remaining amine molecules and decomposition of the material.

- (23) Smith, M. E. *Annu. Rep. NMR Spectrosc.* **2001**, *43*, 121.
- (24) Hartmann, S. R.; Hahn, E. L. *Phys. Rev.* **1962**, *128*, 2042.
- (25) Levitt, M. H.; Suter, D.; Ernst, R. R. *J. Chem. Phys.* **1986**, *84*, 4243.
- (26) Peersen, O. B.; Wu, X.; Kustanovich, I.; Smith, S. O. *J. Magn. Reson. Ser. A* **1993**, *104*, 334.
- (27) Peersen, O. B.; Wu, X.; Smith, S. O. *J. Magn. Reson. Ser. A* **1994**, *106*, 127.
- (28) Metz, G.; Wu, X.; Smith, S. O. *J. Magn. Reson. Ser. A* **1994**, *110*, 219.
- (29) Metz, G.; Ziliox, M.; Smith, S. O. *Solid State Nucl. Magn. Reson.* **1996**, *7*, 155.
- (30) Cook, R. L.; Langford, C. H. *Polym. News* **1999**, *24*, 6.
- (31) Lipton, A. S.; Sears, J. A.; Ellis, P. D. *J. Magn. Reson.* **2001**, *151*, 48.
- (32) Fujiwara, T.; Ramamoorthy, A. *Annu. Rep. NMR Spectrosc.* **2006**, *58*, 155.
- (33) Hung, I.; Rossini, A. J.; Schurko, R. W. *J. Phys. Chem. A* **2004**, *108*, 7112.
- (34) Siegel, R.; Nakashima, T. T.; Wasylshen, R. E. *J. Phys. Chem. B* **2004**, *108*, 2218.
- (35) Zhao, X.; Hoffbauer, W.; Schmedt auf der Gunne, J.; Levitt, M. H. *Solid State Nucl. Magn. Reson.* **2004**, *26*, 57.
- (36) Fu, R.; Gunaydin-Sen, O.; Dalal, N. S. *J. Am. Chem. Soc.* **2007**, *129*, 470.
- (37) Samoson, A.; Tuhern, T.; Gan, Z. *Solid State Nucl. Magn. Reson.* **2001**, *20*, 130.
- (38) Stebbins, J. F.; Du, L.-S.; Kroeker, S.; Neuhoff, P.; Rice, D.; Frye, J.; Jakobsen, H. J. *Solid State Nucl. Magn. Reson.* **2002**, *21*, 105.
- (39) Fu, R.; Brey, W. W.; Shetty, K.; Gor'kov, P.; Saha, S.; Long, J. R.; Grant, S. C.; Chekmenev, E. Y.; Hu, J.; Gan, Z.; Sharma, M.; Zhang, F.; Logan, T. M.; Brueschweller, R.; Edison, A.; Blue, A.; Dixon, I. R.; Markiewicz, W. D.; Cross, T. A. *J. Magn. Reson.* **2005**, *177*, 1.
- (40) Gan, Z.; Gor'kov, P.; Cross, T. A.; Samoson, A.; Massiot, D. *J. Am. Chem. Soc.* **2002**, *124*, 5634.

- (41) Albeniz, A. C.; Barbera, J.; Espinet, P.; Lequerica, M. C.; Levelut, A. M.; Lopez-Marcos, F. J.; Serrano, J. L. *Eur. J. Inorg. Chem.* **2000**, 133.
- (42) Penner, G. H.; Liu, X. L. *Prog. Nucl. Magn. Reson. Spectrosc.* **2006**, *49*, 151.
- (43) Smith, G.; Thomasson, J. H.; White, J. M. *Aust. J. Chem.* **1999**, *52*, 317.

**[Ag(4-pyridinesulfonate)]<sub>4</sub> Reacted with C<sub>12</sub>H<sub>25</sub>NH<sub>2</sub> in 1:1, 1c.** Yield: 93%. Anal. calcd for AgC<sub>17</sub>H<sub>29</sub>N<sub>2</sub>SO<sub>3</sub> (451.37 g/mol): C, 45.24; H, 6.92; N, 6.21. Found: C, 44.65; H, 6.73; N, 6.01. DSC/TGA: 95 °C (12.0 J g<sup>-1</sup>, endo), 103 °C (4.7 J g<sup>-1</sup>, endo), 128 °C (39.9 J g<sup>-1</sup>, endo), 145–215 °C (70.5 J g<sup>-1</sup>, exo), 215–280 °C (116.5 J g<sup>-1</sup>, endo), –22.0% obsd and –41.1% calcd for a loss of 1.0 equiv C<sub>12</sub>H<sub>25</sub>NH<sub>2</sub> in the first two mass losses combined, 280–406 °C (111.2 J g<sup>-1</sup>, endo; 9.2 J g<sup>-1</sup>, endo), loss of the remaining amine molecules and decomposition of the material.

**[Ag(4-pyridinesulfonate)]<sub>4</sub> Reacted with C<sub>12</sub>H<sub>25</sub>NH<sub>2</sub> in 1:1.5, 1d.** Yield: 97%. Anal. calcd for AgC<sub>23</sub>H<sub>44.5</sub>N<sub>2.5</sub>SO<sub>3</sub> (544.05 g/mol): calcd: C, 50.78; H, 8.24; N, 6.44. Found: C, 50.69; H, 8.28; N, 6.40. DSC/TGA: 96 °C (15.6 J g<sup>-1</sup>, endo), 108 °C (66.7 J g<sup>-1</sup>, endo), 115 to 250 °C (77.9 J g<sup>-1</sup>, exo), –32.4% obsd and –51.1% calcd for loss of 1.5 C<sub>12</sub>H<sub>25</sub>NH<sub>2</sub>, 255 to 415 °C (139.2 J g<sup>-1</sup>, endo; 50.9 J g<sup>-1</sup>, endo), loss of remaining amine and decomposition of the material.

**[Ag(4-pyridinesulfonate)]<sub>4</sub> Reacted with C<sub>12</sub>H<sub>25</sub>NH<sub>2</sub> in 1:2, 1e.** Yield: 95%. Anal. calcd for AgC<sub>29</sub>H<sub>54</sub>N<sub>3</sub>SO<sub>3</sub> (632.69 g/mol): C, 55.05; H, 8.60; N, 6.64. Found: C, 55.12; H, 8.77; N, 6.45. DSC/TGA: 95 °C (16.6 J g<sup>-1</sup>, endo), 114 °C (66.7 J g<sup>-1</sup>, endo), 115–254 °C (94.2 J g<sup>-1</sup>, exo), –37.9% obsd and –58.3% calcd for loss of 2.0 C<sub>12</sub>H<sub>25</sub>NH<sub>2</sub>, 254–416 °C (152.2 J g<sup>-1</sup>, endo; 96.9 J g<sup>-1</sup>, endo), loss of the remaining amine and decomposition of the material.<sup>13,15,41</sup>

**Solid-State NMR.** All samples were finely powdered and packed into 5 mm outer-diameter zirconium oxide rotors. Solid-state <sup>109</sup>Ag, <sup>15</sup>N, and <sup>13</sup>C CP/MAS and VACP/MAS NMR spectra were acquired using a Varian Infinity Plus NMR spectrometer with an Oxford 9.4 T ( $\nu_0(^1\text{H}) = 400$  MHz) wide bore magnet, operating at resonance frequencies of  $\nu_0(^{109}\text{Ag}) = 18.61$  MHz,  $\nu_0(^{15}\text{N}) = 40.50$  MHz, and  $\nu_0(^{13}\text{C}) = 100.52$  MHz. A Varian-Chemagnetics 5 mm triple-resonance (HXY) MAS probe was used for all experiments. Probe tuning and matching for low-frequency <sup>109</sup>Ag NMR experiments, and acquisition of spectra with reduced acoustic ringing, were accomplished using a Varian low- $\gamma$  tuning box and low- $\gamma$  preamplifier. In addition, <sup>15</sup>N CP/MAS NMR spectra of **1c** and **1e** were acquired on a Bruker 900 MHz spectrometer using a 3.2 mm HX MAS probe at the National Ultrahigh Field NMR Facility for Solids in Ottawa, Ontario, Canada. The two-pulse phase modulation decoupling sequence<sup>44</sup> was used for all of the CP/MAS experiments.

**<sup>1H-109Ag</sup> CP/MAS NMR.** Silver chemical shifts were referenced to a 9 M aqueous solution of AgNO<sub>3</sub> ( $\delta_{\text{iso}} = 0.0$  ppm) by using solid silver methane-sulfonate, AgSO<sub>3</sub>CH<sub>3</sub>, as a secondary reference ( $\delta_{\text{iso}} = 87.2$  ppm).<sup>20</sup> Proton-decoupled <sup>109</sup>Ag VACP/MAS NMR spectra were acquired with spinning rates ( $\nu_{\text{rot}}$ ) ranging from 2.0 to 8.0 kHz, and calibrated recycle times between 6 and 20 s. Proton  $\pi/2$  pulse widths ranged between 3.75 and 5.5  $\mu\text{s}$ . Hartmann–Hahn matching<sup>24</sup> fields of  $\nu_1(^1\text{H}) = 16.8$  and 27.8 kHz were applied with optimized contact times of 30 or 35 ms. In one special case, proton-decoupled <sup>109</sup>Ag{<sup>1</sup>H} Bloch decay (single-pulse) experiments were acquired, using a 60° pulse width of 8  $\mu\text{s}$  and a recycle delay of 300 s. Additional experimental parameters and details are summarized in Table S1 (Supporting Information).

**<sup>1H-15N</sup> CP/MAS NMR.** Nitrogen chemical shifts were referenced to liquid NH<sub>3</sub> (20 °C),  $\delta_{\text{iso}} = 0$  ppm, by setting the chemical shift of the ammonium peak of a doubly labeled solid <sup>15</sup>NH<sub>4</sub><sup>15</sup>NO<sub>3</sub> (98% <sup>15</sup>N) sample to 23.8 ppm.<sup>45</sup> The <sup>1H-15N</sup> CP/MAS NMR spectra at 9.4 T were acquired at  $\nu_{\text{rot}} = 5$  or 6 kHz with an optimized recycle delay of 4 s. A proton  $\pi/2$  pulse width of 3.75  $\mu\text{s}$  and a

contact time of 2 ms were used, with the collection of between 64 to 152 transients. The <sup>1H-15N</sup> CP/MAS NMR spectra at 21.1 T were acquired with  $\nu_{\text{rot}} = 10$  kHz and a recycle delay of 20 s. A proton  $\pi/2$  pulse width of 2.5  $\mu\text{s}$  and contact time of 2 ms were utilized, with 1024 transients collected in each experiment. Additional experimental parameters are summarized in Table S2 (Supporting Information).

**<sup>1H-13C</sup> CP/MAS NMR.** <sup>1H-13C</sup> CP/MAS NMR spectra have been acquired for most of the systems for purposes of probing sample identity and purity; relevant spectra are included in the Supporting Information (Figures S1–S3). Carbon chemical shifts were referenced to the high-frequency chemical shift of solid adamantane ( $\delta_{\text{iso}} = 38.57$  ppm with respect to tetramethylsilane). Spectra with two different spinning speeds were acquired for each sample, and optimized recycle delays of 6 to 12 s were applied. Additional experimental details are summarized in Table S3 (Supporting Information).

**Spectral Simulations.** Silver chemical shift parameters were obtained via simulations of experimental spectra using the WSolids software package.<sup>46</sup>

**Ab Initio Calculations.** Ab initio calculations of chemical shielding and *J*-coupling tensors were performed using Gaussian 03<sup>47</sup> on Dell precision workstations running Red Hat Linux as well as on Alpha and Opteron workstations on SHARCNET.<sup>48</sup> All of the calculations were performed using the Restricted Hartree–Fock (RHF) method with the valence double- $\zeta$  plus polarization (DZVP) basis set<sup>49</sup> on both the silver and nitrogen atoms<sup>50</sup> and 6-311G\*\* on all of the other atoms. Molecular coordinates used in the calculations on **1a**<sup>15</sup> and on [Ag(NH<sub>3</sub>)<sub>2</sub>]<sub>2</sub>SO<sub>4</sub> (**4**)<sup>51</sup> were taken from the crystal structure data, and those used in the calculations on **1e** and **2b** are based on a structure similar to that reported by Smith et al.<sup>43</sup> In all cases, hydrogen atom positions were geometry-optimized, using the 6-311G\*\* basis set on all H atoms. The nuclear magnetic shielding tensors were calculated using the gauge-including atomic orbitals method.<sup>52,53</sup>

## Results and Discussion

In this section, we will first discuss the <sup>1H-109Ag</sup> CP/MAS NMR spectra of the parent compound **1a**, along with similar spectra of samples **1b–1e**, which are obtained from the reaction of **1a** with stoichiometric amounts of amine. Then, <sup>15</sup>N CP/MAS NMR data are discussed for **1c** (1:1) and **1e** (1:2), in an effort to further refine our understanding of the layered solids. Third, <sup>109</sup>Ag and <sup>15</sup>N NMR data are presented

(46) Eichele, K.; Wasylishen, R. E. *WSolids1: Solid-State NMR Spectrum Simulation*, v. 1.17.30, 2001.

(47) Frisch, M. J. et al. *Gaussian 03*, Rev. B.03; Gaussian, Inc.: Pittsburgh, PA, 2003.

(48) This work was made possible by the facilities of the Shared Hierarchical Academic Research Computing Network (SHARCNET: www.sharcnet.ca).

(49) Basis sets were obtained from the Extensible Computational Chemistry Environment Basis Set Database, V, as developed and distributed by the Molecular Science Computing Facility, Environmental and Molecular Sciences Laboratory, which is part of the Pacific Northwest Laboratory, P.O. Box 999, Richland, Washington 99352, and funded by the U.S. Department of Energy. The Pacific Northwest Laboratory is a multiprogram laboratory operated by Battelle Memorial Institute for the U.S. Department of Energy under contract DE-AC06-76RLO 1830. Contact Karen Schuchardt for further information.

(50) Godbout, N.; Salahub, D. R.; Andzelm, J.; Wimmer, E. *Can. J. Chem.* **1992**, *70*, 560.

(51) Zachwieja, U.; Jacobs, H. Z. *Kristallogr.* **1992**, *201*, 207.

(52) Ditchfield, R. *Mol. Phys.* **1974**, *27*, 789.

(53) Wolinski, K.; Hinton, J. F.; Pulay, P. *J. Am. Chem. Soc.* **1990**, *112*, 8251.

(44) Bennett, A. E.; Rienstra, C. M.; Auger, M.; Lakshmi, K. V.; Griffin, R. G. *J. Chem. Phys.* **1995**, *103*, 6951.

(45) Schurko, R. W.; Wasylishen, R. E. *J. Phys. Chem. A* **2000**, *104*, 3410.

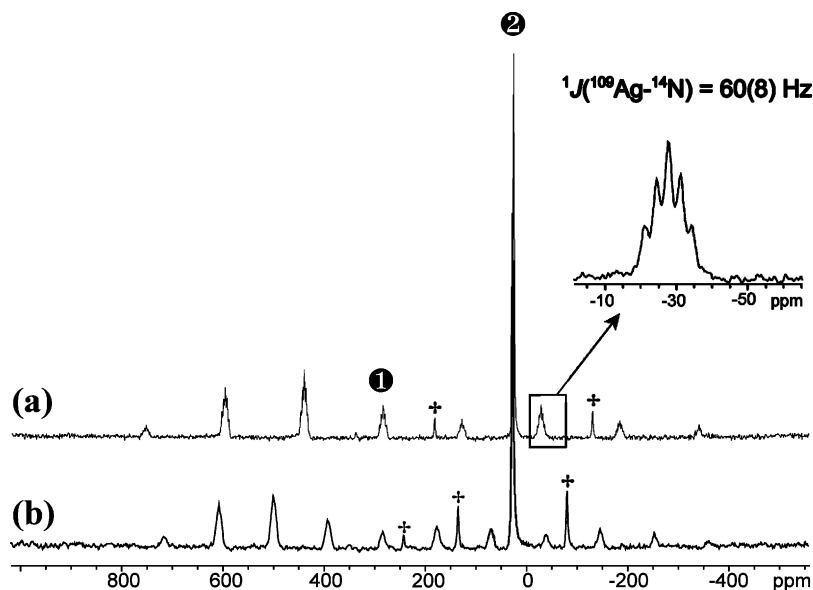


**Figure 1.** Solid-state  $^{109}\text{Ag}$  CP/MAS NMR spectra of **1a** at two different spinning speeds, (a)  $\nu_{\text{rot}} = 2.9$  kHz and (b)  $\nu_{\text{rot}} = 2.0$  kHz. Isotropic peaks for the two distinct silver sites are designated as 1 and 2. The + designates spinning sidebands for site 2; all other peaks are sidebands of site 1.

**Table 1.** Experimental  $^{109}\text{Ag}$  Chemical Shift Parameters<sup>a</sup>

compounds	$\delta_{\text{iso}}$ (ppm) <sup>b</sup>	$\Omega$ (ppm) <sup>c</sup>	$\kappa$ <sup>d</sup>
<b>1a</b> (site 1)	283(2)	1163(50)	0.74(5)
<b>1a</b> (site 2)	25(2)		
<b>1b</b> (site 1)	283(2)		
<b>1b</b> (site 2)	25(2)		
<b>1b</b> (site 3)	508(2)	991(50)	0.95(5)
<b>1c</b> (site 1)	283(2)	1128(50)	0.90(5)
<b>1c</b> (site 2)	25(2)		
<b>1c</b> (site 3)	508(2)	991(50)	0.95(5)
<b>1d</b> (site 1)	283(2)	1106(50)	0.99(1)
<b>1d</b> (site 2)	25(2)		
<b>1d</b> (site 3)	507(2)	1031(50)	0.99(1)
<b>1e</b>	507(2)	1031(50)	0.96(4)
<b>2a</b>	46(1)		
<b>2b</b>	457(2)	1497(50)	0.96(4)
<b>2c</b>	474(2)	1530(50)	0.99(1)
<b>3</b>	454(2)	1322(50)	0.99(1)

<sup>a</sup> The CS tensor is described by three principle components ordered such that  $\delta_{11} \geq \delta_{22} \geq \delta_{33}$ . <sup>b</sup>  $\delta_{\text{iso}} = (\delta_{11} + \delta_{22} + \delta_{33})/3$ . <sup>c</sup>  $\Omega = \delta_{11} - \delta_{33}$ . <sup>d</sup>  $\kappa = 3(\delta_{22} - \delta_{\text{iso}})/\Omega$ .

for a different series of layered materials, **2a–2c**, and compared to the first series of materials, as well as to  $[\text{Ag}(\text{C}_{12}\text{H}_{25}\text{NH}_2)_2]^+[\text{NO}_3]^-$  (**3**). Finally, a thorough discussion of ab initio calculations of silver and nitrogen chemical shift tensors and silver–nitrogen  $J$ -couplings and their use in defining and proposing a structural model for the layered solids is presented.

**[Ag(4-pyridinesulfonate)]<sub>4</sub> (1a).**  $^1\text{H}$ - $^{109}\text{Ag}$  CP/MAS NMR spectra of **1a** acquired at two MAS speeds (Figure 1) reveal two peaks with isotropic chemical shifts of 283 and 25 ppm (silver CS parameters are summarized in Table 1). The two shifts indicate the presence of two crystallographically distinct silver sites, in agreement with the known crystal structure of **1a**.<sup>15</sup> Since the Ag(1) nucleus, the pyridine ligated center, is in a nearly linear environment (N–Ag–N = 168.62°) and the Ag(2) nucleus, the sulfonate ligated center, is in a distorted tetrahedral environment (Scheme 1), the assignment of the resonances is straightforward. Ag(1) should have a significantly larger CSA than Ag(2), since the magnetic shielding is distinct in directions parallel and

perpendicular to the N–Ag–N bonding arrangement. On the other hand, Ag(2) is in a relatively spherically symmetric environment by comparison, and the CSA is reduced. Therefore, Ag(1) and Ag(2) are assigned to the peaks at 283 and 25 ppm, respectively. Herzfeld–Berger analysis<sup>54</sup> was used to extract the silver CS tensor parameters for site 1 using the slow-spinning spectrum (2.0 kHz), yielding a span and skew of  $\Omega = 1163$  ppm and  $\kappa = 0.74$ , respectively. The skew indicates that the shielding tensor is nearly axially symmetric, from which it may be inferred that the distinct component,  $\delta_{33}$ , is directed along or near the direction of the N–Ag–N bonding arrangement. An accurate CS tensor cannot be obtained from the small manifold of sidebands for Ag(2), but an upper limit of  $\Omega = 250$  ppm can be estimated from ab initio calculations (vide infra), which is comparable to experimentally measured silver CS tensors for Ag nuclei in five- and six-coordinate silver atoms in  $\text{AgSO}_3\text{CH}_3$  (183.4(5) ppm) and  $[\text{Ag}(p\text{-toluenesulfonate})]$  (163(4) ppm), respectively.<sup>21</sup>

The  $^{109}\text{Ag}$  NMR spectrum acquired at  $\nu_{\text{rot}} = 2.9$  kHz (Figure 1a) was processed with less line broadening than the slow-spinning spectrum, and fine structure is clearly visible. Closer examination of the pattern with  $\delta_{\text{iso}} = 283$  ppm reveals a quintet of 1:2:3:2:1 intensity (Figure 1, inset), which arises from indirect spin–spin coupling between  $^{109}\text{Ag}$  and two  $^{14}\text{N}$  nuclei,  $^1J(^{109}\text{Ag}, ^{14}\text{N})$ , where  $^{14}\text{N}$  is a spin  $I = 1$  nucleus (n.a. = 99.63%). The magnitude of  $^1J(^{109}\text{Ag}, ^{14}\text{N})$ , 60(8) Hz (Table 2), is typical for a silver atom bound to an  $\text{sp}^2$  nitrogen.<sup>21</sup>

**Complex 1a reacted with  $\text{C}_{12}\text{H}_{25}\text{NH}_2$  in Ratios of 1:0.5, 1:1, 1:1.5, and 1:2 (1b, 1c, 1d, and 1e).** The  $^1\text{H}$ - $^{109}\text{Ag}$  CP/MAS NMR spectra of **1b**, **1c**, **1d**, and **1e** are compared to the parent sample, **1a**, in Figure 2. As the loading level of the dodecylamine is increased, a new spinning sideband manifold emerges with a distinct isotropic shift (ca. 507 ppm). The intensity of this pattern increases with increasing

(54) Herzfeld, J.; Berger, A. E. *J. Chem. Phys.* **1980**, *73*, 6021.

**Table 2.** Experimental Indirect Spin–Spin Couplings

compounds	$^1J(^{109}\text{Ag},^{14}\text{N})$ (Hz)	$^1J(^{109}\text{Ag},^{15}\text{N})$ (Hz) <sup>a</sup>	$^1K(\text{Ag},\text{N})$ <sup>b</sup> ( $\text{N A}^{-2} \text{m}^{-3}$ )
<b>1a</b> (site 1)	60(8)		$-1.47663 \times 10^{22}$
<b>1e</b>		61(8)	$1.07023 \times 10^{22}$
<b>2b</b>	50(8)	70(5)	$-1.23053 \times 10^{22}$
<b>2c</b>	50(8)		$-1.23053 \times 10^{22}$
<b>3</b>	50(8)		$-1.23053 \times 10^{22}$

<sup>a</sup> Values of  $^1J(^{109}\text{Ag},^{15}\text{N})$  were measured from  $^{109}\text{Ag}$  and  $^{15}\text{N}$  NMR spectra of labeled complexes. <sup>b</sup> Reduced couplings were calculated using (ref 60)  $K_{XY} = 4\pi^2 J_{XY} / h\gamma_X\gamma_Y$ .

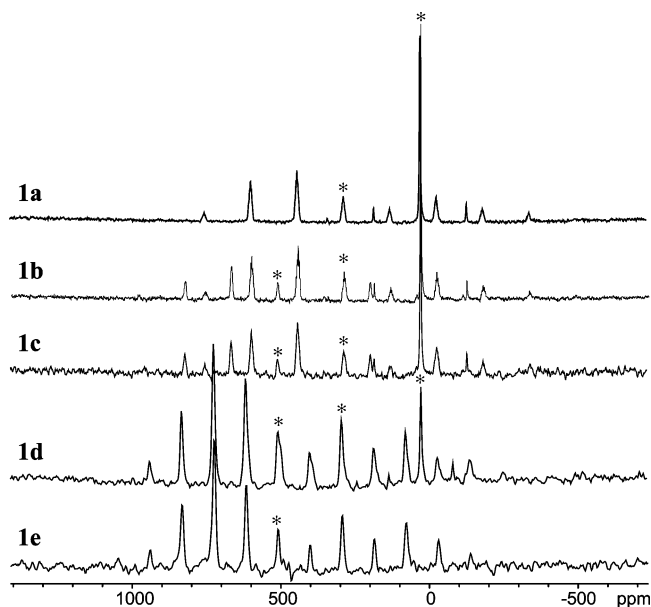


**Figure 2.** Solid-state  $^{109}\text{Ag}$  CP/MAS NMR spectra of **1a**–**1e**. Isotropic peaks are designated with asterisks (\*). Spectra of **1a**, **1b**, and **1c** were acquired at  $\nu_{\text{rot}} = 2.9$  kHz and spectra of **1d** and **1e** were acquired at  $\nu_{\text{rot}} = 2.0$  kHz.

amine loading level until only this pattern remains (**1e**). Silver CS tensor parameters extracted from the lower-spinning speed powder patterns of **1e** are  $\delta_{\text{iso}} = 507$  ppm,  $\Omega = 1031$  ppm, and  $\kappa = 0.96$  (Figure 3a,b). The higher-frequency shift (i.e., the  $^{109}\text{Ag}$  nucleus is deshielded relative to those in the parent compound), in combination with the span and skew, suggests the existence of a distinct silver environment from those of **1a**.  $^1\text{H}$ - $^{109}\text{Ag}$  CP/MAS NMR spectra of **1e** were also acquired at a higher spinning speed ( $\nu_{\text{rot}} = 8.0$  kHz), revealing triplets of 1:2:1 intensity (Figure 3c). The size of the splitting is ca. 61(8) Hz, indicating that the  $^{109}\text{Ag}$  nucleus is  $J$ -coupled to two  $^{15}\text{N}$  nuclei in the  $\text{sp}^3$  environments of the dodecylamines. The distinct multiplets arising from  $J$ -coupling to  $^{14}\text{N}$  nuclei of the pyridine rings are not observed, indicating that silver–pyridine nitrogen bonds are absent. The data indicate that, at loadings above one equivalent of amine, the primary species present involves a major reconstruction of the coordination polymer backbone. The higher loadings of amine may enable a requisite degree of swelling to allow the transformation, may displace the pyridine ligands directly, or may likely lead to some combination of the two factors. Clearly, simple intercalation of the primary amine is not the only process occurring; rather, what is being

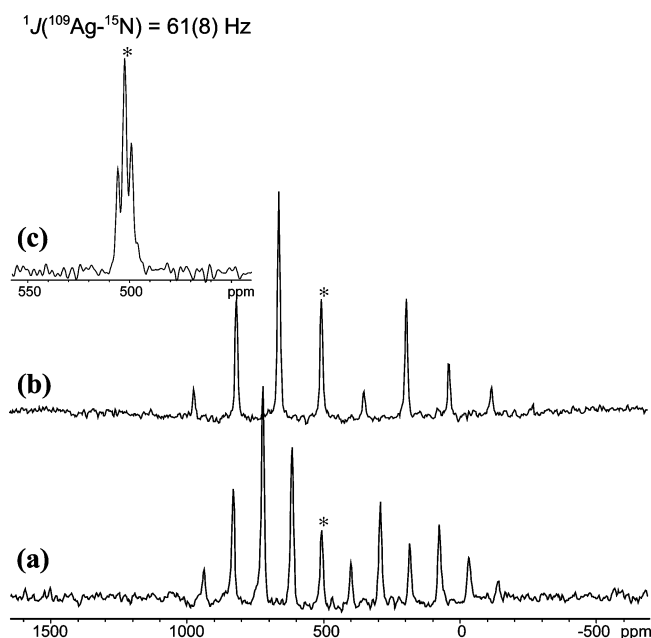


**Figure 3.** Solid-state  $^{109}\text{Ag}$  CP/MAS NMR spectra of **1e** at three different spinning speeds: (a)  $\nu_{\text{rot}} = 2.0$  kHz, (b)  $\nu_{\text{rot}} = 2.9$  kHz, (c)  $\nu_{\text{rot}} = 8.0$  kHz. Isotropic peaks are designated with asterisks (\*).

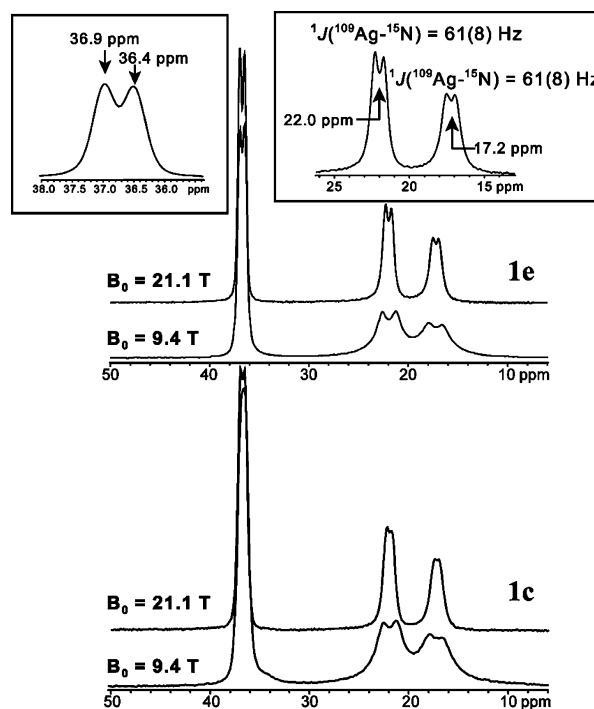


**Figure 4.**  $^{15}\text{N}$  CP/MAS NMR spectra of **1c** (1:1) and **1e** (1:2) acquired at two different fields. The doublets around 36 ppm (shown in the inset) correspond to different nitrogen sites of free amines. The doublets at 17 and 22 ppm correspond to nitrogen sites coupled to silver atoms. The insets are expansions taken from **1e**.

witnessed is the gradual formation of **1e**, which has a new silver coordination site.

$^1\text{H}$ - $^{15}\text{N}$  CP/MAS NMR experiments were conducted on **1c** and **1e** at 9.4 and 21.1 T (Figure 4, Table 3). The spectra are essentially identical, unlike their distinct  $^{109}\text{Ag}$  NMR spectra. In the  $^{15}\text{N}$  NMR spectra acquired at 9.4 T, there are two higher-frequency peaks at 36.9 and 36.4 ppm, and two lower-frequency peaks centered at 22.0 and 17.2 ppm, the latter of which are

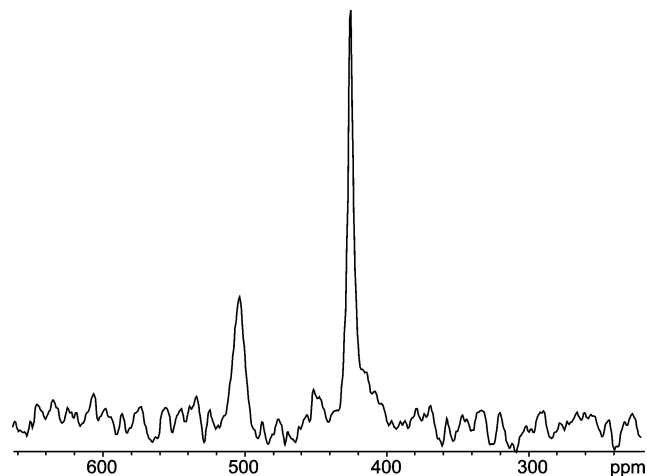
**Table 3.** Experimental  $^{15}\text{N}$  Chemical Shifts

compounds	$\delta_{\text{iso}}$ (ppm) of coordinated nitrogen	$\delta_{\text{iso}}$ (ppm) of uncoordinated nitrogen
<b>1c</b>	21.9(5), 17.2(5)	36.9(5), 36.5(5)
<b>1e</b>	21.9(5), 17.2(5)	36.9(5), 36.4(5)
<b>2b</b>	19.4(5), 14.0(5)	minor species, 36.6(5) ppm

split due to  $^1J(^{109}\text{Ag},^{15}\text{N}) = 61(8)$  Hz, in agreement with splittings measured in the corresponding  $^{109}\text{Ag}$  NMR spectra of **1e**. Due to the similarity of gyromagnetic ratios of  $^{107}\text{Ag}$  and  $^{109}\text{Ag}$ , the  $^1J(^{107}\text{Ag},^{15}\text{N})$  and  $^1J(^{109}\text{Ag},^{15}\text{N})$  could not be differentiated. Integration of the  $^{15}\text{N}$  CP/MAS NMR spectra of both samples reveals intensity ratios of 1:1 between these two regions (this was assessed under multiple contact times). The shifts and integrated intensities of all of the peaks, as well as the  $J$ -coupling observed for the low-frequency resonances, were confirmed by experiments conducted at 21.1 T, since the difference in hertz for the peaks split by  $J$ -coupling is constant regardless of the field strength, and easily differentiated from peaks with different chemical shifts, which are constant in parts per million. The high-frequency peaks have similar isotropic shifts to “free” dodecylamine<sup>55</sup> (vide infra) and indicate the presence of a noncoordinated amine species. The low-frequency,  $J$ -split peaks are assigned to nitrogen atoms of the dodecylamine, which are interacting with silver atoms in the newly formed material.<sup>22,41,56</sup> Coordinative displacement of sulfonate ligands by high loadings of amines has been observed.<sup>57</sup> This assignment is consistent with the numerous negative coordination shifts,  $\Delta\delta = \delta_{\text{iso}}^{\text{coord}} - \delta_{\text{iso}}^{\text{free}}$ , reported for the coordination of amine ligands to transition metals.<sup>45,58,59</sup>

These data confirm the notion that **1e** is gradually being formed from **1a** and dodecylamine. Previous XRD experiments<sup>15</sup> conducted at room and higher temperatures for **1c** and **1e** were proposed to reveal the “reversible” release of amine and the regeneration of **1a** for the former, while such behavior was not observed for the latter. It is possible that the combination of “free” dodecylamine released upon heating **1c**, along with the remaining unreacted **1a**, gave the impression that a reversible intercalation of the amine was occurring. In fact, the disparate set of  $^{109}\text{Ag}$  NMR spectra and identical set of  $^{15}\text{N}$  NMR spectra for these samples demonstrate that samples **1b**, **1c**, and **1d** are likely simple mixtures of **1a** and **1e**.

However, this does raise some questions regarding the formation of **1e** from **1a**. Aside from the highly selective reaction at the silver site, which requires cleavage of two sub-2.0 Å Ag–pyridyl bonds in **1a** and replacement by two amine molecules, it is likely that the amine is playing a role in exfoliating the layers of **1a** and “bowing” the layers such that the silver sites are exposed to reaction with the primary amines. Such layer bending has been observed for more rigid

**Figure 5.** Solid-state  $^{109}\text{Ag}\{^1\text{H}\}$  MAS NMR spectrum of **1e** at 9.4 T,  $\nu_{\text{rot}} = 8.0$  kHz.

molecular sheets such as those in graphite.<sup>60</sup> Unfortunately, the formation of a layered solid phase consisting of **1a** and intercalated amine would be very difficult to distinguish by NMR from **1a** and free amine and may only exist transiently during the formation of **1e**. While the formation of a transitory layered solid en route to the formation of **1e** is plausible, and is somewhat consistent with the  $^{109}\text{Ag}$  NMR data, the  $^{15}\text{N}$  NMR spectra strongly suggest the constant presence of **1a** and **1e**.

Complex **1e** is clearly not an intercalation solid, and its structure must now be considered. Since **1e** is known to have a layered structure from powder XRD patterns,<sup>15</sup> and based on known structures of analogous silver systems, it is possible that the silver–diamine cations form bilayers.<sup>41,61</sup> However, since sample **1e** has a 1:2 ratio of silver atoms to dodecylamines, it seems that half of the silver sites are unaccounted for in this model. It is possible that the  $^1\text{H}$ - $^{109}\text{Ag}$  CP/MAS NMR experiments are unable to detect silver sites which are not proximate to an abundant proton source. Hence, lengthy  $^{109}\text{Ag}\{^1\text{H}\}$  Bloch-decay MAS NMR experiments, run with a recycle time of 300 s, reveal a sharp peak at 425 ppm (Figure 5) with no fine structure ( $\Delta\nu_{1/2} = 78$  Hz), which was not observed in previously discussed  $^1\text{H}$ - $^{109}\text{Ag}$  CP/MAS NMR spectra. The silver resonance at 507 ppm in this spectrum, corresponding to the amine-coordinated silver, is broad and more difficult to observe. The new peak has a shift similar to those observed for silver sites in  $\text{Ag}_2\text{SO}_3$  (between 409 and 466 ppm),<sup>21</sup> likely corresponding to an isolated, uncoordinated silver ion. We are cautious in our definition of “isolated” in this case: by *isolated*, we refer to a Ag site which is not strongly coordinated by oxygen atoms (as in **1a**), and there are no coordination shifts indicating hydrogen bonding, nor fine structure to indicate the presence of nearby NMR active nuclides. Unfortunately, the integrated intensities of these peaks (isolated/coordinated, 1.5:1.0) are not quantitatively representative of the amount of silver, since the  $^{109}\text{Ag}$  relaxation time constants are different for each site,

(55) Antonelli, D. M. *Microporous Mesoporous Mater.* **1999**, *30*, 315.(56) Drew, M. G. B.; Farrell, D.; Morgan, G. G.; McKee, V.; Nelson, J. *Dalton* **2000**, 1513.(57) Liu, P.; Lian, Z.-X.; Cai, J. *Polyhedron* **2006**, *25*, 3045.(58) Mason, J. *Chem. Rev.* **1981**, *81*, 205.(59) Witanowski, M.; Stefaniak, L.; Webb, G. A. *Annu. Rep. NMR Spectrosc.* **1986**, *18*, 1.(60) Zabel, H.; Kamitakahara, W. A.; Nicklow, R. M. *Phys. Rev. B* **1982**, *26*, 5919.(61) Neve, F.; Ghedini, M.; Demunno, G.; Levelut, A. M. *Chem. Mater.* **1995**, *7*, 688.

and part of the broader, high-frequency signal is lost due to the rapidly decaying FID. In fact, the  $T_2$  associated with the broad resonance is so short that this resonance is not observed in Hahn echo experiments with interecho delays of  $\tau = 125$   $\mu$ s; hence, only Bloch decay experiments could be applied.

If the silver-diamine cations form bilayers, then the “free” dodecylamine molecules, silver ions, and pyridinesulfonate counteranions are likely positioned between the layers, or perhaps among the alkyl chains of the dodecylamines;<sup>41,43,61</sup> however, no interactions of these species with the diamine cations are detected, and the precise arrangement of these species is unknown at this time. The structural positioning of the uncoordinated dodecylamines could potentially be very interesting, as they could be located among the layers in a variety of scenarios. In addition, they may play a role in the gradual conversion of **1a** to **1e** with the addition of amine, since the 1:1 reaction does not completely form a new layered solid.

Solid-state NMR spectra indicate that the structure of **1e** is very different from that of **1a**: in the former, the silver atom is strongly coordinated to two dodecylamine nitrogen atoms, as opposed to the nitrogen atoms in the pyridine–sulfonate moieties in the latter. The increased axial symmetry of the silver CS tensor also indicates that the N–Ag–N arrangement of atoms is increasingly linear in **1e** in comparison to that in **1a**. A reaction has occurred in which half of the dodecylamine molecules coordinate to silver atoms to form silver diamine cations, while the remaining dodecylamine molecules do not have strong bonding interactions with silver atoms. A structural model is further developed below, via comparison to data for other samples, as well as through theoretical calculations on model systems.

**Ag(*p*-toluenesulfonate) (2a) and 2a reacted with C<sub>12</sub>H<sub>25</sub>NH<sub>2</sub> and C<sub>9</sub>H<sub>19</sub>NH<sub>2</sub> in 1:2 ratios (2b and 2c).** The <sup>1</sup>H-<sup>109</sup>Ag CP/MAS NMR spectrum of **2a** has one sharp (fwhh of 100 Hz), isotropic peak at 46 ppm (Figure 6a). This isotropic shift is the same as per Penner and Li, who also reported silver CS tensor parameters of  $\Omega = 163$  ppm and  $\kappa = 0.15$ .<sup>21</sup> The observation of one peak for this sample is consistent with the crystal structure, since the four silver atoms in the unit cell are related by an inversion center and are therefore chemically and magnetically equivalent. The arrangement of atoms around the silver site is described as trigonal prismatic, featuring five oxygen atoms and two other silver atoms as nearest neighbors.<sup>13</sup> The structure of **2a** is distinct from that of **1a** in that the inorganic and organic moieties are not contained within the same layer (Scheme 1); thus, **2a** is classified as a hybrid inorganic–organic solid, with the toluene moieties “pendant” into the interlayer region.<sup>13</sup>

Sample **2a** was reacted with two equivalents of unlabeled dodecylamine and nonylamine to produce **2b** and **2c**, respectively.<sup>13</sup> The <sup>109</sup>Ag CP/MAS NMR spectrum of **2b** has a single isotropic peak at 457 ppm, flanked by a large set of spinning sidebands (Figure 6b). The span is very large,  $\Omega = 1497$  ppm, and the CS tensor is axially symmetric,  $\kappa = 0.96$ . Once again, the high-frequency shift and CS tensor characteristics indicate that the silver is in a linear or near-

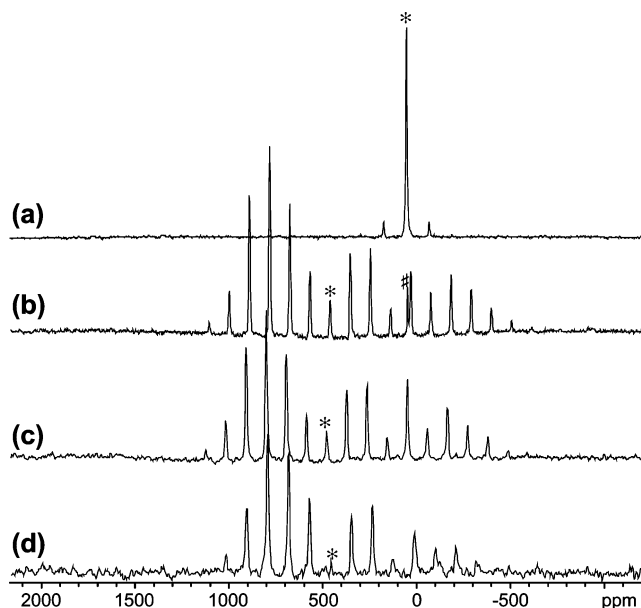


**Figure 6.** Solid-state <sup>1</sup>H-<sup>109</sup>Ag CP/MAS NMR spectra of (a) **2a**, (b) **2b**, (c) **2c**, and (d) **3** at  $\nu_{\text{rot}} = 2.0$  kHz. Isotropic peaks are denoted with asterisks (\*); remaining peaks are spinning sidebands. The # denotes an impurity from the starting material, **2a**.

linear environment, suggesting the formation of a diamine cation. The <sup>109</sup>Ag CP/MAS NMR spectrum of **2b** acquired at  $\nu_{\text{rot}} = 2.9$  kHz, and processed with no additional line broadening and two zero fills, provides enough resolution to identify 1:2:3:2:1 multiplets with  $^1J(^{109}\text{Ag}, ^{14}\text{N}) = 50(8)$  Hz (Figure 7a), confirming the proposed cation formation. Similar results are observed for **2c** (Figure 6c), demonstrating that the alkyl chain lengths do not have much influence on the <sup>109</sup>Ag NMR parameters. Prior work indexing the powder XRD patterns of a nonylamine intercalate was consistent with a layered AgRSO<sub>3</sub> network where the amine defined the interlayer region; however, as for the first series of compounds, it was not possible to determine the nature of the amine’s interaction with the layers.<sup>13</sup>

A sample of **2b** was made with <sup>15</sup>N-labeled dodecylamine to confirm the binding of the dodecylamine to the silver sites. The <sup>1</sup>H-<sup>109</sup>Ag CP/MAS NMR spectrum of the labeled **2b** reveals a single silver site with a spinning sideband pattern identical to that of the unlabeled sample, with the exception of the presence of 1:2:1 triplets and  $^1J(^{109}\text{Ag}, ^{15}\text{N}) = 70(5)$  Hz (Figure S4, Supporting Information). The <sup>1</sup>H-<sup>15</sup>N CP/MAS spectrum of the labeled **2b** (Figure 8) indicates that most of the dodecylamine is involved in direct coordination to silver sites, with  $\delta_{\text{iso}}$  of 19.4(5) and 14.0(5) ppm, and  $^1J(^{109}\text{Ag}, ^{15}\text{N})$  matching the corresponding <sup>109</sup>Ag NMR spectrum. However, unlike in the case of **1e**, there is not a 1:1 ratio of coordinated and uncoordinated amine. The peak at 36.6 ppm corresponding to “free” amine is of very low integrated intensity and now corresponds to a mere impurity, along with several other peaks, which are separate from or underlying the main resonances at 19 and 14 ppm.

**[Ag(C<sub>12</sub>H<sub>25</sub>NH<sub>2</sub>)<sub>2</sub>]<sup>+</sup>[NO<sub>3</sub>]<sup>-</sup> (3).** Further understanding of the structures of **2b** and **2c** can be made by considering the **[Ag(C<sub>12</sub>H<sub>25</sub>NH<sub>2</sub>)<sub>2</sub>]<sup>+</sup>[NO<sub>3</sub>]<sup>-</sup> (**3**) coordination compound. It has been proposed that the silver diamine cations of **3** consist of**



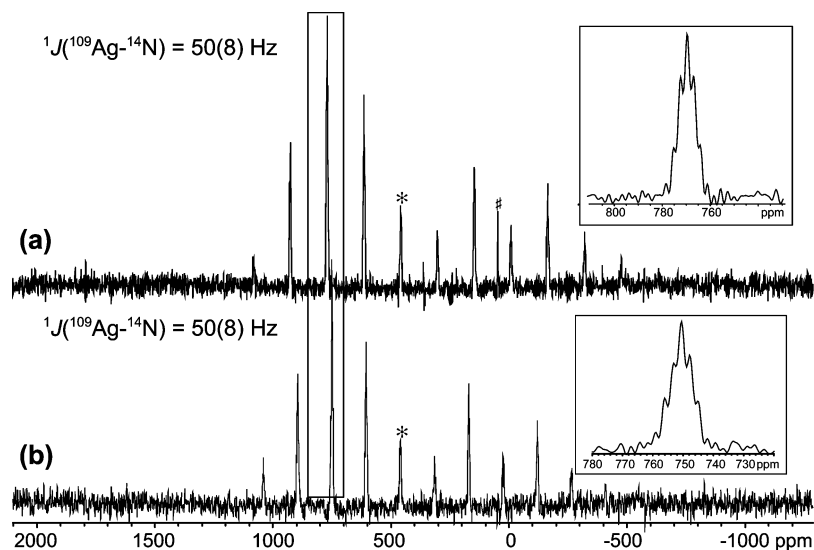


**Figure 7.** High-resolution solid-state  $^{109}\text{Ag}$  CP/MAS NMR spectra of (a) **2b** and (b) **3** (both processed with two zero-fills). Isotropic peaks are denoted by asterisks (\*), and insets are expansions of areas indicated by rectangles. The # denotes an impurity from the starting material, **2a**.

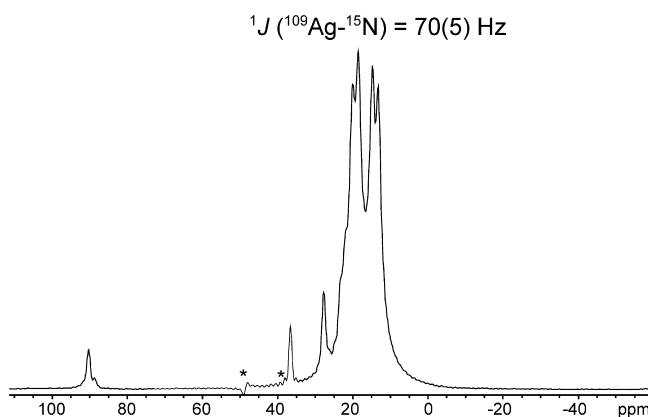


**Figure 8.**  $^1\text{H}$ - $^{15}\text{N}$  CP/MAS NMR spectrum of **2b**. The doublets at 14 and 19 ppm correspond to nitrogen sites coupled to silver atoms. The peak at 36 ppm corresponds to a small amount of unreacted dodecylamine. The low intensity peaks at 27 and 90 ppm correspond to some impurity from the  $^{15}\text{N}$  labeled dodecylamine sample. Low intensity peaks in the region of 20 to 30 ppm underlie the main resonances, and can be attributed to either dodecylamines in differing environments or perhaps impurity phases. The asterisks denote an artifact resulting from Fourier transforming a truncated FID, which was necessary to minimize the high-power decoupling and acquisition times.

$\text{N}-\text{Ag}-\text{N}$  in a near-linear arrangement, and alkyl chains which adopt a “U-shape”, resulting in self-assembly into a bilayered structure.<sup>41,61</sup> The  $^1\text{H}$ - $^{109}\text{Ag}$  CP/MAS NMR spectrum of **3** (Figure 6d) looks remarkably like those of **2b** and **2c**, with  $\delta_{\text{iso}} = 454$  ppm,  $\Omega = 1322$  ppm, and  $\kappa = 0.99(1)$ .  $^1\text{H}$ - $^{109}\text{Ag}$  CP/MAS NMR experiments on unlabeled **3** at  $\nu_{\text{rot}} = 2.7$  kHz and processed with two zero fills and minimal line broadening (Figure 7b) reveal 1:2:3:2:1 multiplets with  $^1J(^{109}\text{Ag},^{14}\text{N}) = 50(8)$  Hz, confirming that each silver is bonded to two dodecylamine molecules.

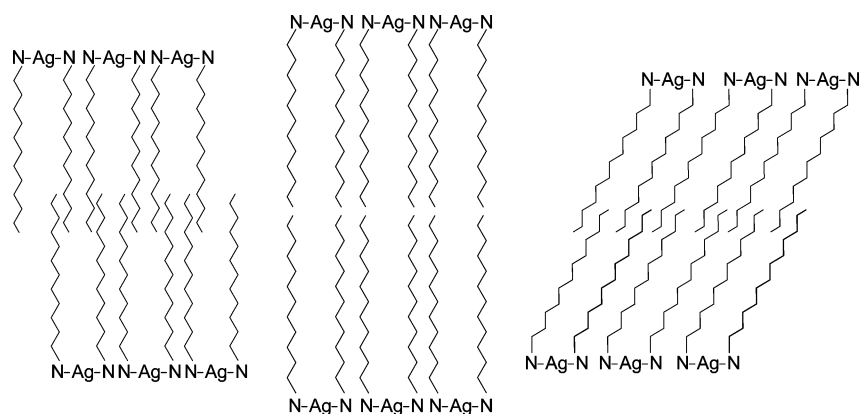
The similarity of the silver chemical shift tensors and  $J$ -coupling parameters of **2b**, **2c**, and **3** suggests that they have comparable structures, with silver atoms in linear  $\text{N}-\text{Ag}-\text{N}$  arrangements. The  $^{109}\text{Ag}$  and  $^{15}\text{N}$  NMR data, along with powder XRD data on **1e** and **2b**, suggest that the structures of **1e**, **2b**, **2c**, and **3** all consist of silver–diamine cations which adopt the proposed “U-shaped” structures and

form bilayers (Scheme 2). The “free” dodecylamines do not seem to be necessary for the stabilization or formation of the layered structures, except in the case of **1e**. The positions of additional species (including anions for all species and “free” dodecylamines for **1e**) cannot be directly probed with the  $^{109}\text{Ag}$  or  $^{15}\text{N}$  NMR experiments, though theoretical structural modeling may be utilized to shed further light on these structural aspects.

**Ab Initio Calculations.** First principles calculations of silver and nitrogen chemical shielding tensors, as well as  $^1J(^{109}\text{Ag},^{14}\text{N})$  coupling constants, can be readily performed with modern computational chemistry suites such as Gaussian 03. In this section, we first present calculations of silver CS tensor parameters and  $J$ -coupling constants on a model compound for a well-characterized structure,  $[\text{Ag}(\text{NH}_3)_2]_2\text{-SO}_4$ , in order to determine which method and basis sets yield the best agreement between experiment and theory, as well as to establish an approximate chemical shift scale (no absolute chemical shielding standard has been reported for silver to date). Second, calculations of NMR interactions of structural models for **1a** are presented (Figure 9a,b), since it has two well-characterized, distinct silver sites. Third, we discuss the computation of NMR parameters for  $[\text{Ag}(\text{NH}_2\text{R})_2]^+$  units (Figure 10, Table S4, Supporting Information), which are used as structural models for **1e** and **2b** (Figure 9c,d). A preliminary exploration into the potential environments of additional species, including “free” or noncoordinated amine and organic sulfonate anions, is also presented.

$[\text{Ag}(\text{NH}_3)_2]_2\text{SO}_4$  is a reasonable starting model compound for choosing an appropriate method and basis sets, since it has a known crystal structure<sup>51</sup> and silver CS tensor parameters and  $^1J(^{109}\text{Ag},^{14}\text{N})$  coupling constants have been measured.<sup>22</sup> Following Bowmaker et al., the model cluster  $[(\text{Ag}(\text{NH}_3)_2)_3(\text{HSO}_4)_2]^+$  (**I**) is investigated, using geometry optimized protons on the sulfonate groups. The silver atom is coordinated to two  $\text{sp}^3$ -nitrogen atoms, similar to that in **1e** and **2b**. The RHF method, with DZVP basis sets<sup>49</sup> on

**Scheme 2.** A Schematized Representation Showing Possible Layered Arrangements (Interdigitated, Noninterdigitated, and Angled Interdigitated) of the U-Shaped Silver-Dodecylamine Cations in the Structures of **1e** and **2b**<sup>a</sup>



<sup>a</sup> Uncoordinated silver cations, amines, and pyridinesulfonate groups are omitted. Three-dimensional extension of these structures back into the page are omitted for clarity.

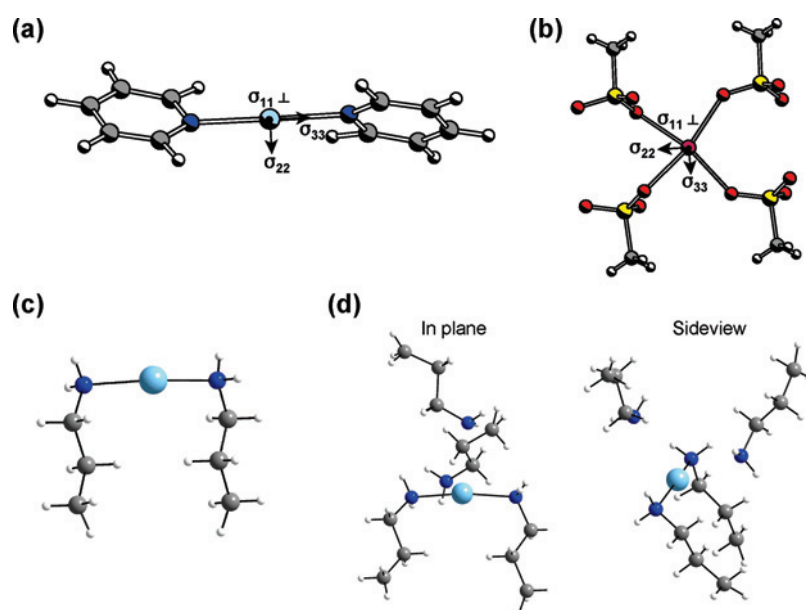


**Figure 9.** Theoretically calculated silver chemical shielding tensor orientations in structural models for **1a** at sites (a) Ag(1) (model structure **II**) and (b) Ag(2) (**III**) and structural models for (c) **2b** ( $[\text{Ag}(\text{NH}_2\text{C}_3\text{H}_7)_2]^+$ , **IV**) and (d) **1e** ( $[\text{Ag}(\text{NH}_2\text{C}_3\text{H}_7)_2]^+ \cdot 2(\text{NH}_2\text{C}_3\text{H}_7)$ , **VI**).

silver and nitrogen atoms<sup>49,50</sup> and 6-311G\*\* on all other atoms, yields the best agreement with experimentally measured silver CS tensors and  $^1J(^{109}\text{Ag}, ^{14}\text{N})$  (Table 4, Table S5, Supporting Information), producing results similar to those of Bowmaker and co-workers,<sup>22</sup> who used DFT calculations with the ADF suite, including zeroth-order relativistic approximation.<sup>22</sup>

To further test the consistency of the choice of method and basis sets, similar calculations were conducted on model systems for **1a**. The structural unit used to model site Ag(1) in **1a** consists of a silver atom bonded to two pyridine rings,  $\{\text{Ag}[\text{py}]_2\}^+$  (**II**, Figure 9a), in which the sulfonate groups are replaced by hydrogen atoms to reduce computational expense. The calculated values of  $\Omega$  and  $\kappa$  are in good agreement with experimental data, and the CS tensor is oriented such that  $\sigma_{33}$  (the most shielded component) is near the Ag–N bonds ( $\angle\sigma_{33}\text{–Ag–N1} = 5.75^\circ$  and  $\angle\sigma_{33}\text{–Ag–N2} = 5.64^\circ$ ). The skew is not axially symmetric, since the N–Ag–N angle is not exactly  $180^\circ$ , and  $\sigma_{11}$  and  $\sigma_{22}$  are oriented in different environ-

ments, as predicted from experimental results. However, the theoretical value of  $^1J(^{109}\text{Ag}, ^{14}\text{N})$  is less than the experimental value, and the isotropic shift is not accurately reproduced. The structural model for site Ag(2),  $[\text{Ag}(\text{SO}_3\text{Me})_4]^{3-}$  (**III**, Figure 9b), is also based on the crystal structure; however, to reduce computational expense, the pyridine moieties on the sulfur atoms were replaced by methyl groups. There are no experimental silver CS tensor data for this site; however, we found that, by setting  $\delta_{\text{iso}} = 25$  ppm (the experimental value) for the Ag(2) site, the relative chemical shift values of all of the other model compounds scaled well with experimental values. This is by no means an endorsement of this particular model as an absolute chemical shielding standard; a detailed experimental and theoretical determination of such a standard is beyond the scope of this paper.

The  $^{109}\text{Ag}$  and  $^{15}\text{N}$  NMR spectra of **1e** and **2b** indicate that the silver sites are coordinated to two dodecylamines; hence, one of the structural models used for these species is

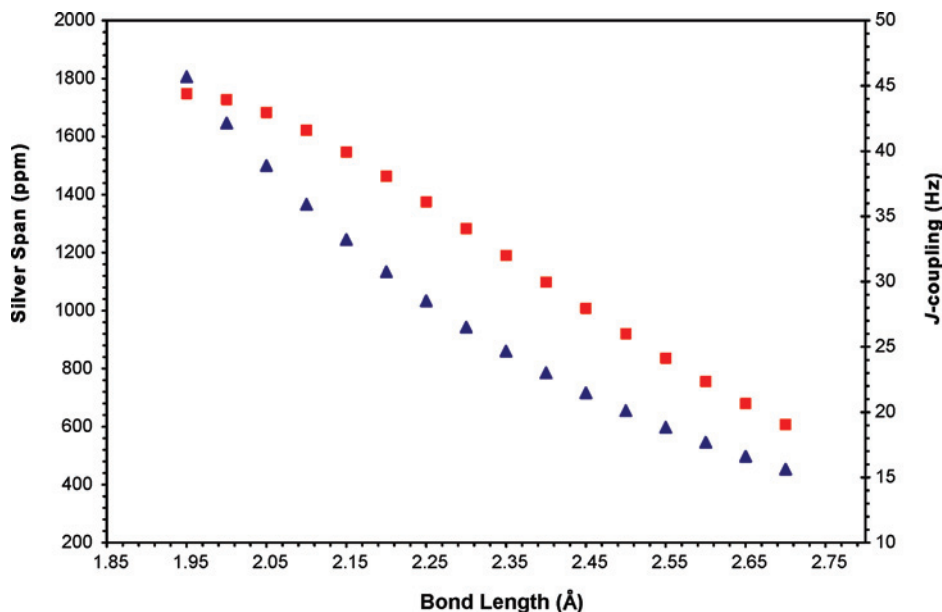


**Figure 10.**  $^1J(^{109}\text{Ag}, ^{14}\text{N})$  coupling (■) and span (▲) as a function of Ag–N bond length in  $[\text{Ag}(\text{NH}_2\text{C}_3\text{H}_7)]^+$ .

**Table 4.** Experimental and Theoretical  $^{109}\text{Ag}$  Chemical Shift Parameters and  $^1J(^{109}\text{Ag}, ^{14}\text{N})$  Coupling Values

structural unit <sup>a</sup>	$r(\text{Ag}-\text{N})$ (Å)	$\sigma_{\text{iso}}$ (ppm)	$\delta_{\text{iso}}$ (ppm) <sup>b,c</sup>	$\Omega$ (ppm)	$\kappa$	$^1J(^{109}\text{Ag}, ^{14}\text{N})$ (Hz)
[Ag(NH <sub>3</sub> ) <sub>2</sub> ] <sub>2</sub> SO <sub>4</sub> (sample <b>4</b> )						
experimental	2.11		657(2)	1708(50)	0.62(5)	47(8)
$[\text{Ag}(\text{NH}_3)_2(\text{HSO}_4)_2]^{+d}$ ( <b>I</b> )	2.11	3546	657	1652	0.84	41
Ag(PS) (sample <b>1a</b> )						
experimental (site 1)	2.16		283(2)	1163(50)	0.74(5)	60(8)
$[\text{Ag}(\text{py})_2]^+$ ( <b>II</b> )	2.16	3988	215	1100	0.87	38
experimental (site 2)			25(2)			
$[\text{Ag}(\text{SO}_3\text{Me})_4]^{3-}$ ( <b>III</b> )		4174	29	257	−0.53	
sample <b>2b</b>						
experimental			457(2)	1395(50)	0.92(5)	50(8)
$[\text{Ag}(\text{NH}_2\text{C}_3\text{H}_7)_2]^+$ ( <b>IV</b> )	2.10	3729	474	1366	0.93	42
$[\text{Ag}(\text{NH}_2\text{C}_6\text{H}_{13})_2]^+$ ( <b>V</b> )	2.10	3728	475	1370	0.93	42
sample <b>1e</b>						
experimental			507(2)	1031(50)	0.96(4)	43(8)
$[\text{Ag}(\text{NH}_2\text{C}_3\text{H}_7)_4]^{+e}$ ( <b>VI</b> )	2.10	3652	526	1231	0.83	38
$[\text{Ag}(\text{NH}_2\text{C}_3\text{H}_7)_4]^{+e}$ ( <b>VI</b> )	2.15	3741	452	1096	0.83	35

<sup>a</sup> The model structure formulae and reference numbers (in boldface Roman numerals) are listed below. <sup>b</sup> The chemical shifts were calculated using  $\delta_{\text{iso}}(\text{sample}) - \delta_{\text{iso}}(\text{ref}) = \sigma_{\text{iso}}(\text{ref}) - \sigma_{\text{iso}}(\text{sample})$  where  $\delta_{\text{iso}}(\text{ref})$  and  $\sigma_{\text{iso}}(\text{ref})$  are the  $^{109}\text{Ag}$  experimental chemical shift and the calculated chemical shielding, respectively. <sup>c</sup> The  $\delta_{\text{iso}}$  of the Ag(2) site of **1a** was set to 25 ppm as an approximate chemical shift reference. See text for details. <sup>d</sup> This unit is taken from the reported crystal structure with the addition of two hydrogen atoms to avoid the negative charge. <sup>e</sup> The positions of the uncoordinated amines were optimized.

$[\text{Ag}(\text{NH}_2\text{C}_3\text{H}_7)_2]^+$  (**IV**, Figure 9c). The starting model for **IV** was constructed from a crystal structure reported by Smith et al.,<sup>43</sup> with optimized proton positions. In order to reduce computational expense, the alkyl chains only have three carbons; this feature of our model is justified by aforementioned  $^{109}\text{Ag}$  NMR data for **2b** and **2c**, as well as calculations on  $[\text{Ag}(\text{NH}_2\text{C}_6\text{H}_{13})_2]^+$  (**V**, not pictured), both of which reveal that CS and  $J$ -coupling parameters are not influenced to any great degree by chain length differences.

Different structural parameters were varied in order to observe corresponding changes in NMR parameters. The variation of the silver CS span and  $^1J(^{109}\text{Ag}, ^{14}\text{N})$  as a function of internuclear distance (Figure 10, Table S4, Supporting Information) reveals that both  $\Omega$  and  $^1J(^{109}\text{Ag}, ^{14}\text{N})$  increase with decreasing Ag–N bond lengths; this behavior is expected for the latter, since its magnitude is dominated by the Fermi-contact mechanism and increasing  $s$  character in

the Ag–N bond.<sup>62</sup> The best agreement between the theoretical silver CS tensor parameters and those of **2b** is observed at  $r(\text{Ag}-\text{N}) = 2.10$  Å (Table S4, Supporting Information), while  $^1J(^{109}\text{Ag}, ^{14}\text{N})$  is slightly underestimated. This value of  $r(\text{Ag}-\text{N})$  is a reasonable equilibrium bond length for this structure, since there are a number of analogous molecules having Ag–N( $\text{sp}^3$ ) bond distances of ca. 2.1 Å<sup>22,51,63–65</sup> and similar values of  $^1J(^{109}\text{Ag}, ^{14}\text{N})$ .<sup>22</sup>

While model structure **IV** may be adequate for describing **2b**, the parameters are clearly distinct from **1e**, and simple geometrical adjustments to the  $[\text{Ag}(\text{NH}_2\text{C}_3\text{H}_7)_2]^+$  coordinates (Ag–N bonds, as well as  $\angle(\text{N}-\text{Ag}-\text{N})$  and  $\angle(\text{C}-\text{N}-\text{N}-\text{C})$ , Tables S6 and S7, Supporting Information) are insufficient for modeling this system. Hence, calculations were conducted on numerous structural models, which include additional

(62) Jameson, C. J. In *Multinuclear NMR*; Mason, J., Ed.; Plenum Press, New York, 1987, p 639.

**Table 5.** Calculated  $^{15}\text{N}$  Isotropic Chemical Shielding Values and Associated Coordination Shifts Relative to Free Propylamine in the Structural Models for **1e**

structural unit	Ag–N (Å)	$\sigma_{\text{iso}}$ (ppm)	$\Delta\delta^a$	
[Ag(NH <sub>2</sub> C <sub>3</sub> H <sub>7</sub> ) <sub>2</sub> ] <sup>+</sup>	2.10	273.7	–22.0	
	2.15	271.0	–19.3	
	2.20	268.5	–16.8	
[Ag(NH <sub>2</sub> C <sub>3</sub> H <sub>7</sub> ) <sub>4</sub> ] <sup>+</sup> <sup>b</sup> (site 1)	2.10	272.2	–20.8	
	2.10	268.5	–17.1	
	(site 2)	2.90	251.6	0.2
	(site 3)	3.02	250.4	1.1
[Ag(NH <sub>2</sub> C <sub>3</sub> H <sub>7</sub> ) <sub>4</sub> ] <sup>+</sup> <sup>b</sup> (site 1)	2.15	269.8	–18.2	
	(site 2)	2.15	266.2	–14.7
	(site 3)	2.90	252.0	–0.1
	(site 4)	3.02	250.7	0.9

<sup>a</sup>  $\Delta\delta = \delta_{\text{iso}}^{\text{coord}} - \delta_{\text{iso}}^{\text{free}}$ , where  $\delta_{\text{iso}}^{\text{coord}}$  is the  $^{15}\text{N}$  chemical shift of the nitrogen site coordinated to the silver atom and  $\delta_{\text{iso}}^{\text{free}}$  is the  $^{15}\text{N}$  chemical shift of free propylamine. The RHF/6-311G\*\* nitrogen  $\sigma_{\text{iso}}$  for propylamine is 251.7 ppm. The coordination shift is defined as  $\Delta\delta \approx -\Delta\sigma$ . <sup>b</sup> The position of the third amine was geometry-optimized in this calculation.

noncoordinated amine units and pyridine sulfonate ions, all of which exert considerable influence on the CS tensors and  $J$ -couplings (see the Supporting Information). Interestingly, fairly good agreement was found in structural models incorporating two additional propylamine units which are weakly coordinated (through geometry optimization) to the silver atom, [Ag(NH<sub>2</sub>C<sub>3</sub>H<sub>7</sub>)<sub>2</sub>]<sup>+</sup>·2(NH<sub>2</sub>C<sub>3</sub>H<sub>7</sub>) (Figure 9d, **VI**). Specifically, calculations involving Ag–N bonds of 2.10 and 2.15 Å, and weakly coordinated amines with Ag–N distances of 2.9 and 3.1 Å, yield reasonably good agreement with experimental data for **1e**, suggesting that weaker, long-range interactions are key in determining the silver tensor characteristics, and hence, influencing its overall structure.

Theoretical nitrogen chemical shifts are also of use in modeling the structure of **2b** (Table 5). Our experimental results indicate a coordination shift,  $\Delta\delta = \delta_{\text{iso}}^{\text{coord}} - \delta_{\text{iso}}^{\text{free}}$ , of between ca. –15 and –20 ppm in **1e** and between ca. –14 and –22 ppm in **2b**. Calculations are in excellent agreement, predicting coordination shifts of  $\Delta\delta = -16$  to –22 ppm for the coordination of two propylamine molecules to silver to form the cationic diamine complex. As expected, calculations predict that additional long-range interactions between silver and propylamines will yield no noticeable change in isotropic chemical shift, with  $\Delta\delta$  ranging from –0.2 to +1.0 ppm.

Ab initio calculations of silver CS tensors, silver–nitrogen  $J$ -couplings, and nitrogen coordination shifts are all useful in the elucidation of the local structure of the silver-dodecylamine cations in layered systems like **2b**. However, for systems like **1e**, in which there may be additional long-range interactions, the structures are more difficult to model on the basis of NMR data; further investigations and structural refinement are required. It is possible that molecular dynamics/annealing simulations combined with first prin-

ciples calculations of silver and nitrogen NMR tensors may be useful for future elucidation of the structures of these complex materials; notably, the nature of the long-range layered structure and counteranion positions.

## Conclusions

Layered silver supramolecular frameworks reacted with primary amines have been characterized using SSNMR, powder XRD, and ab initio calculations.  $^{109}\text{Ag}$  and  $^{15}\text{N}$  NMR spectroscopy have been utilized to demonstrate that new materials (**1e** and **2b**) are formed which consist of silver diamine cations, counteranions, and, in the case of **1e**, “free” amine molecules and uncoordinated silver sites. Amines are crucial in the formation of these materials as both noncoordinative guests and highly selective reactants at the silver sites.  $^{109}\text{Ag}$  and  $^{15}\text{N}$  NMR data, along with complementary NMR parameters obtained from ab initio calculations, unequivocally demonstrate the formation of silver diamine cations and the disappearance of the original metal-organic frameworks. The combined powder XRD and NMR data suggest that the silver diamine cations are responsible for forming a bilayered structure. Though the positions of the counteranions are somewhat ambiguous, ab initio calculations demonstrate that additional amines that are weakly coordinated to the silver sites may influence the silver CS tensors while not producing an observable  $J$ -coupling and suggest that these amines may be crucial in stabilizing the layered structure of **1e**. In a broader view, this study demonstrates the importance of combining complementary physical characterization methods for obtaining a more comprehensive understanding of molecular structure underlying new materials.

**Acknowledgment.** R.S., H.H., A.L., L.M., and G.S. would like to thank the Natural Science and Engineering Research Council (NSERC, Canada) for research funding. R.S. and H.H. also thank the Canadian Foundation for Innovation (CFI), the Ontario Innovation Trust (OIT), and the University of Windsor for funding the solid-state NMR facility. The Centre for Catalysis and Materials Research (CCMR) at the University of Windsor is also acknowledged for support. H.H. thanks the Ministry of Training, Colleges and Universities for an Ontario Graduate Scholarship and UW for a Tuition Scholarship. We would also like to thank Dr. Victor Tersikh and Dr. Shane Pawsey for acquiring  $^{15}\text{N}$  NMR spectra at 21.1 T at the National Ultrahigh-field NMR Facility for Solids in Ottawa, Ontario, Canada. Ab initio computations were carried out using the Shared Hierarchical Academic Research Computing Network (SHARCNET: www.sharcnet.ca).

**Supporting Information Available:** Complete ref 47, detailed experimental parameters and coordinates of the atoms in the proposed models used for the calculation of  $^{109}\text{Ag}$  and  $^{15}\text{N}$  CS tensor parameters of **1e**, and  $^{13}\text{C}$  NMR data. This material is available free of charge via the Internet at <http://pubs.acs.org>.

IC801549P

(63) You, Z. L.; Zhu, H. L.; Liu, W. S. *Acta Crystallogr., Sect. E* **2004**, E60, m1903.

(64) You, Z. L.; Yang, L.; Zou, Y.; Zeng, W. J.; Liu, W. S.; Zhu, H. L. *Acta Crystallogr., Sect. C* **2004**, C60, m117.

(65) You, Z. L.; Zhu, H. L.; Liu, W. S. *Acta Crystallogr., Sect. C* **2004**, C60, m231.